Biofouling

The Journal of Bioadhesion and Biofilm Research

ISSN: 0892-7014 (Print) 1029-2454 (Online) Journal homepage: http://www.tandfonline.com/loi/gbif20

Development and evaluation of an experimental protocol for 3-D visualization and characterization of the structure of bacterial biofilms in porous media using laboratory X-ray tomography

Tomislav Ivankovic, Sabine Rolland du Roscoat, Christian Geindreau, Philipe Séchet, Zhujun Huang & Jean M. F. Martins

To cite this article: Tomislav Ivankovic, Sabine Rolland du Roscoat, Christian Geindreau, Philipe Séchet, Zhujun Huang & Jean M. F. Martins (2016) Development and evaluation of an experimental protocol for 3-D visualization and characterization of the structure of bacterial biofilms in porous media using laboratory X-ray tomography, Biofouling, 32:10, 1235-1244, DOI: 10.1080/08927014.2016.1249865

To link to this article: http://dx.doi.org/10.1080/08927014.2016.1249865

Published online: 09 Nov 2016.

BIOFOULING, 2016
VOL. 32, NO. 10, 1235–1244
http://dx.doi.org/10.1080/08927014.2016.1249865

Taylor & Francis
Taylor & Francis Group

Development and evaluation of an experimental protocol for 3-D visualization and characterization of the structure of bacterial biofilms in porous media using laboratory X-ray tomography

Tomislav Ivankovic[a,b,c], Sabine Rolland du Roscoat[a], Christian Geindreau[a], Philipe Séchet[c], Zhujun Huang[c] and Jean M. F. Martins[d]

[a]Laboratoire 3SR, Université Grenoble-Alpes/CNRS/G-INP, UMR 5521, Grenoble, France; [b]Division of Microbiology, Department of Biology, Faculty of Science, University of Zagreb, Zagreb, Croatia; [c]Laboratoire LEGI, Université Grenoble-Alpes/CNRS/G-INP, UMR 5519, Grenoble, France; [d]Laboratoire LTHE Université Grenoble-Alpes/CNRS/G-INP/IRD, UMR 5564, Grenoble, France

ABSTRACT

The development of a reliable model allowing accurate predictions of biofilm growth in porous media relies on a good knowledge of the temporal evolution of biofilm structure within the porous network. Since little is known about the real 3-D structure of biofilms in porous media, this work was aimed at developing a new experimental protocol to visualize the 3-D microstructure of the inside of a porous medium using laboratory X-ray microtomography. A reliable and reproducible methodology is proposed for (1) growing a biofilm inside a porous medium, and (2) X-ray tomography-based characterization of the temporal development of the biofilm at the inlet of the biofilter. The statistical analysis proposed here also validates the results presented in the literature based on a biofilm structure single measurement.

ARTICLE HISTORY
Received 8 June 2016
Accepted 14 October 2016

KEYWORDS
Biofilter; biofilm; X-ray tomography; *Pseudomonas putida*

Introduction

Bacterial biofilms have started to receive intense research interest in the last decade. In medicine, they are considered as a negative phenomenon because bacteria in biofilms are up to 1,000 times more resistant than planktonic cells to antimicrobials (Stewart & Costerton 2001; Hogan & Kolter 2002) and biofilms associated with implants cause major problems in surgery (Stewart & Costerton 2001; Patenge et al. 2012). In addition, bacteria in the form of a biofilm display increased resistance to disinfectants which results in global spreading of hospital-acquired infections (Bridier et al. 2011; Espinal et al. 2012). On the other hand, bacterial biofilms can be desirable in biotechnology; shorter retention times and increased number of cells in biofilm bioreactors offer advantage over planktonic cells in wastewater treatment (Nicolella et al. 2000; Salama et al. 2015) and the ability to immobilize compounds along with enhanced gene transfer among biofilm occupants facilitates bioremediation (Rajbir et al. 2006).

Biofilms are mainly studied in porous systems such as soils or biofilters in the case of civil engineering and in water and wastewater treatment, bioremediation and filtration in chemical engineering (von der Schulenburg et al. 2009; Iltis et al. 2011). Biofilm growth in porous systems, a process commonly known as bioclogging or biofouling, reduces permeability and induces significant modifications of hydrodynamic properties (Stoodley et al. 2005; Shafahi & Vafai 2009; Karrabi et al. 2011). Hence, suitable numerical 3-D modeling simulations of biofilm growth in such systems are essential to improve industrial processes associated with biofilms. The characterization of biofilm microstructure in porous media represents a key point for the development of efficient macroscopic models of biofilm growth.

Ideally, the models dedicated to biofilm development in a porous medium would be based on experimental data obtained at the microscale (at the biofilm scale), at the mesoscale (at the scale of a few particles of the porous medium) and at the macroscale (the scale of the biofilter). Microscale data on biofilm structure can be obtained by microscopy on planar substrata (confocal, light, electron, atomic force; Beyenal et al. 2004; Billings et al. 2015; Meideros 2016) and macroscale data can be extrapolated from measuring hydrodynamic properties coupled with

CONTACT Sabine Rolland du Roscoat sabine.rollandduroscoat@3sr-grenoble.fr

biomass/biofilm detection (Karrabi et al. 2011). The characterization of the mesoscale, however, remains an unresolved problem. Statistical data at this scale would address the main features of a biofilm, namely its 3-D structure and spatial distribution, at the scale of a pore in the host medium.

Mesoscale characterization therefore requires the direct imaging of biofilms within the porous medium, which is not a simple task. As detailed in a comprehensive review (Beyenal et al. 2004) on methods for quantifying biofilm structures, 'Biofilm researchers hope that the image analysis of biofilms will become a tool that allows the comparison of biofilms grown at different locations and under different growth conditions. It is not certain that this is realistic.' However, there have been initial attempts to visualize biofilms in porous media by using X-ray microtomography (Davit et al. 2011; Iltis et al. 2011). In these two studies microtomography was coupled with the use of suitable contrast agents to differentiate biofilms and the surrounding bulk liquid. Further development of the method involved combining recent advances in synchrotron microtomography and a novel contrast agent, 1-chloronaphtalen (Rolland du Roscoat et al. 2014). All of the above works highlight that further work is necessary.

However, all the work on visualization of biofilms in porous media is based on single experiments (Beyenal et al. 2004; Iltis et al. 2011; Davit et al. 2011; Majumdar et al. 2014), which does not offer a proof for reproducibility of the experiments and therefore on the measurements of biofilm structure.

The work presented here aimed at increasing knowledge of the mesoscale structure of biofilms in porous media through the direct nondestructive 3-D visualization of bacterial biofilms reproducibly grown in a simple porous medium. This study: (1) proposes a reliable and reproducible protocol to grow biofilms in a porous medium (Material and methods section, biofilm growth); (2) extends the methodology based on the 1-chloronaphthalene contrast agent to visualize bacterial biofilms using synchrotron to laboratory X-ray microtomography; and (3) validates the accuracy of the biofilm structure measurement obtained using this methodology.

Materials and methods

Biofilm growth

The mini-biofilters were composed of chromatographic glass columns of 10 mm inner diameter, 15 mm outer diameter and 200 mm in length (XK 13 GC Healthcare Ltd, London, UK) in which glass beads (1 or 2 mm diameter, Assistent, Sondheim, Germany) were introduced. These transparent glass columns and the partly transparent glass beads allowed visual monitoring of the growth dynamics. Moreover, compared to plastic beads that present similar X-ray absorption coefficients to those of biofilms and water, glass beads present very different X-ray absorption properties from water and biofilm, which allowed excellent differentiation (see next section).

To facilitate biofilm formation in the columns, glass beads were colonized with axenic cultures of *Pseudomonas putida* (DSM 6521) in batch systems using the following procedure: prior to each experiment bacterial cells were pre-grown on Luria-Bertani (LB) agar plates (composition in g l^{-1}: casein peptone 10; yeast extract 5; NaCl 5; Agar 20; pH 7.0 ± 0.2) at 30°C for 24 h. From the plate, cell suspension was made (10^8 colony forming units (CFU) ml^{-1}) and 1 ml of suspension was inoculated into 300 ml laboratory bottles containing 100 ml of liquid LB medium.

Next, about 23 g of glass beads were autoclaved (121°C/20 min), added to the bottle and set for incubation at 30°C for 24 h with aeration (1 l min^{-1} of sterile air). During the incubation, the bacterial cells were adsorbed to the surface of the glass beads in the form of a monolayer and in the form of microcolonies. Figure 1 shows the initial spatial repartition of bacteria developed on a glass slide under static conditions prepared as mentioned above. These optical images, which cannot be properly obtained with glass beads, illustrate the initial attachment of bacterial repartition. The amount of adsorbed bacteria was determined by the methodology described by Durham et al. (1994) and amounted 4.1 ± 3.4 × 10^7 CFU g^{-1} of glass beads. The pre-colonized beads were then gently washed with sterile 0.3% NaCl to remove the non-adhering biomass and then transferred into the previously autoclaved columns. The columns were connected to a peristaltic pump (Gilson Minipuls 3, Gilson Inc., Middleton, WI, USA). The tubing (silicone and PTFE capillary tubing, GE Healthcare, Little Chalfont, UK) of the whole system (Figure 2) was autoclaved prior to the start of the experiment. The columns were continuously supplied with the diluted (1/10) LB medium described above since it has been shown that diluted media facilitate biofilm formation in packed media compared to undiluted media (Vogt et al. 2013; Rolland du Roscoat et al. 2014). The O_2 levels of the liquid medium were measured (WTW MultiLine 3430, Weilheim, Germany) in the bottles prior to autoclaving and just after the experiment finished, and ranged from 6.9 to 7.9 mg l^{-1}, depending on the bottle volume. Experiments were performed at room temperature (23 ± 1°C). Several biofilms were grown in parallel over one, five, seven or 10 days at a flow rate of 21.4 ml h^{-1}.

Contrast agent for X-ray tomography

To obtain the 3-D spatial repartition of the constituents of the biofilter, X-ray microtomography scans were

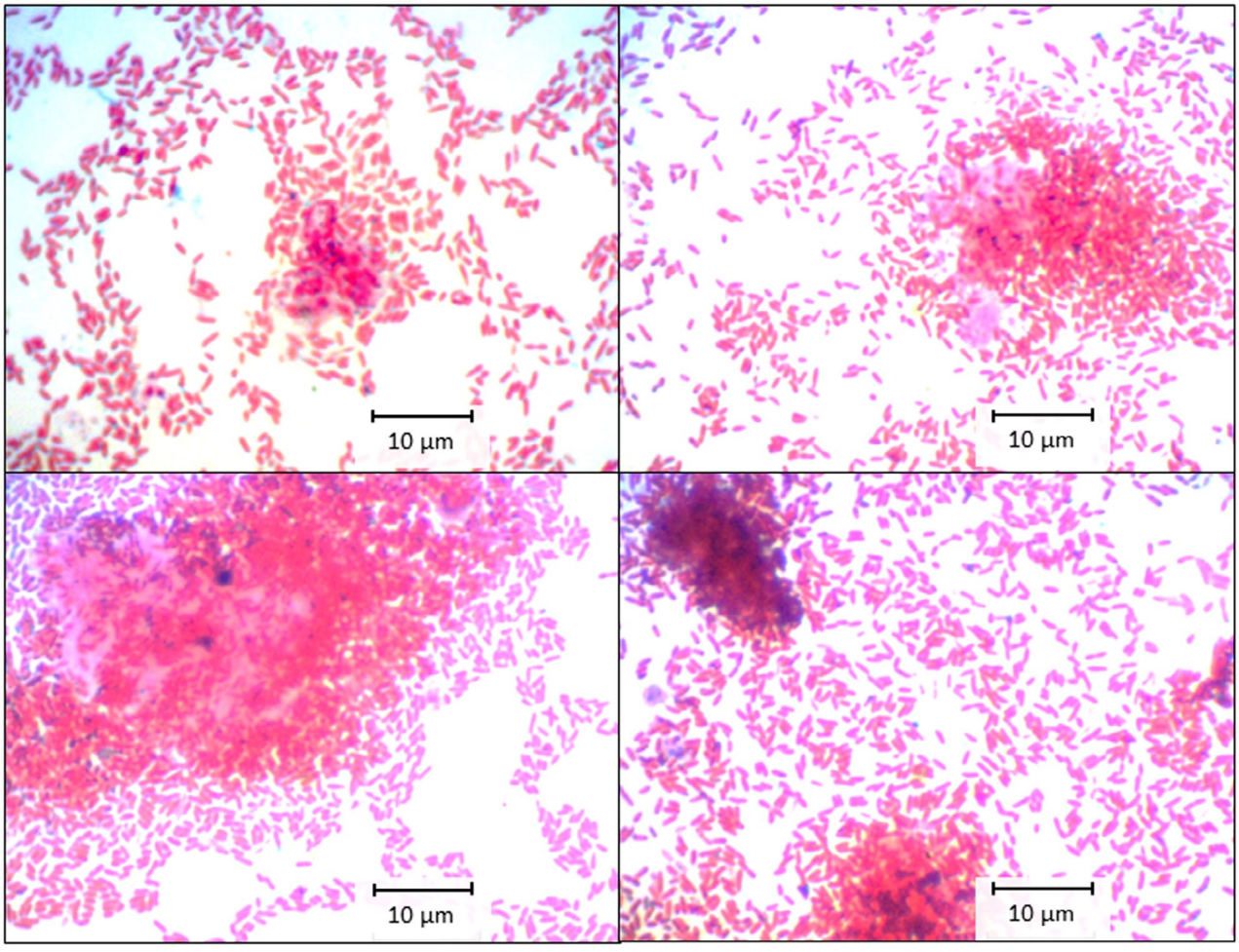

Figure 1. Light microscope images of *P. putida* cells attached to the surface of glass slide after aerobic incubation for 24 h in LB broth at 30°C. Prior to imaging, the slide was gently washed with sterile saline solution, so only attached cells remained. Since the incubation conditions were identical, the same mode of attachment presumably occurred on the surface of the glass beads as well. Gram stain; magnification 1,000 × : Olympus CX21; imaged with Dino-Eye AM423X.

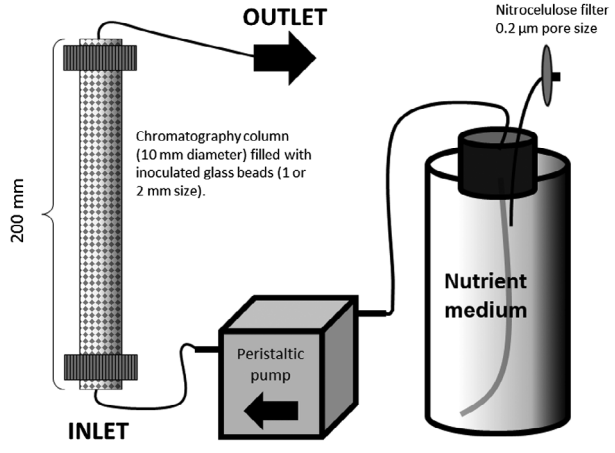

Figure 2. Schematic of the experimental setup used for biofilm growth in a porous medium consisting of chromatography columns filled with glass beads (1 or 2 mm in diameter). The columns were inoculated with a pure culture of *P. putida* and fixed on a stand in order to be continuously fed with nutrient medium with a peristaltic pump for the desired period of time (one to 10 days).

performed. This technique (eg Rolland du Roscoat et al. 2014 in the case of biofilm) gives access to the 3-D structure of the analyzed object. The 3-D datasets represent a 3-D map of X-ray attenuation, that is proportional to the density of the constituents of the sample. Since biofilms and liquid nutrients are very close from a chemical point of view, it is not possible to distinguish the biofilm from the liquid phase. Therefore, the use of a contrast agent to increase the X-ray attenuation of the liquid will allow the liquid and biofilm phases to be identified. The chosen contrast agent (Rolland du Roscoat et al. 2014) was 1-chloronaphthalene (CN). CN is an oily, slightly viscous liquid, the density of which is higher than that of water (1.2 g cm^{-3}).

After the desired time of biofilm growth, the columns were disconnected from the pump system and the contrast agent was introduced. The columns were not emptied prior to injection so that CN extruded and substituted the nutrient medium; CN was injected in the column using a peristaltic pump at a flow rate of 10 ml h^{-1}. The column

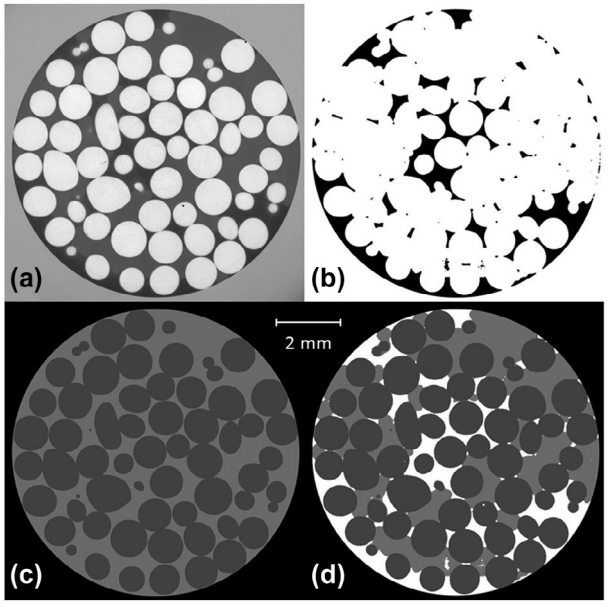

Figure 3. Different segmentation steps in the microtomographs. In the X-ray tomographic images (a) different phases appear in various shades of gray (biofilm = dark gray, 1-chloronaphtalen = light gray, beads = white) which can be separated as biofilm (b) or beads (c). When images are merged (d), each phase is represented by a single color (biofilm = white, beads = dark gray, 1-chloronaphtalen = light gray).

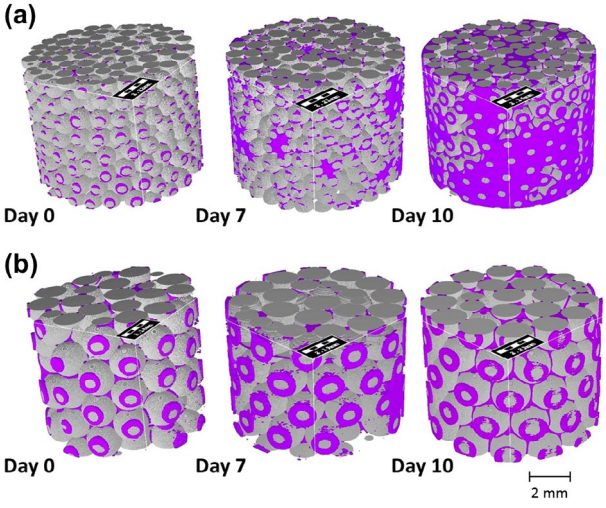

Figure 4. 3-D reconstructions of columns filled with 1 mm (a) and 2 mm beads (b) without biofilm (day 0) and with biofilm grown for seven or 10 days.

was considered to be completely filled with CN when there was no longer any aqueous medium flowing out at the column outlet.

Columns were then inserted into the metallic sample holders to be mounted on the rotation stage of the laboratory tomograph. The mini-biofilters were irradiated with an X-ray beam (generated with a 110 kV 90 µA electron beam on a tungsten target) for 1,200 angular projections equally spaced over 360°. The chosen pixel size of the laboratory microtomography (manufactured by RX Solutions (Annecy, France) with a Hamamatsu L12161-07 source (Hamamatsu City, Japan) and a Varian flat panel detector (Varian Medical Systems, Salt Lake City, UT, USA)) was set to 10 µm px^{-1}. The transmitted beam, which corresponds to 2-D radiographs, was then converted into 3-D datasets using a filtered backprojection algorithm. The scans were undertaken at identical locations for all columns, ie at 20 mm height from the column inlet. The 3-D datasets obtained were gray level 3-D images as illustrated in Figure 3a, with the gray level representing the reconstructed X-ray attenuation coefficient.

Image analysis and biofilm quantification

To quantify the volume fraction of biofilm in the glass bead columns, the three main phases present in the tomographic images need to be unequivocally separated into solid (glass beads), biofilm and liquid (CN) phases. Figure 3 illustrates the different segmentation steps on a slice. The segmentation process was done using Fiji software (https://fiji.sc). The original grayscale images (Figure 3a) were converted into trinary images (black, gray and white) by two consecutive thresholding operations; the threshold was manually chosen. A first threshold was used to separate the solid phase from the porous phase (Figure 3b), and a second one for beads (Figure 3c). A median filter was also applied to each image created in (b) and (c), the size of which was set accordingly to image quality. The two newly created images were then combined by using the 'Image calculator' function to obtain a final image in which each phase is represented by a single color (Figure 3d). The segmented images were then imported into Geodict© software (www.geodict.com), which permits 3-D image reconstructions (Figures 4–6) and enables biofilm quantification. From these segmented images, the 3-D volume fraction of each constituent was deduced by simple counting of the voxels (3-D pixels) that belong to each phase. On numerical images, the volume fraction of biofilm can be obtained by:

$$Biofilm\ volume\ fraction(\%) = \frac{N(biofilm)}{N(biofilm) + N(liquid)} \times 100$$

where N denotes the number of voxels that belong to the phase mentioned between brackets.

Results and discussion

Biofilm growth: visual inspection

Visual inspection of biofilm growth reveals that from days 1 to 3 no growth was apparent in the columns. At days 4–5

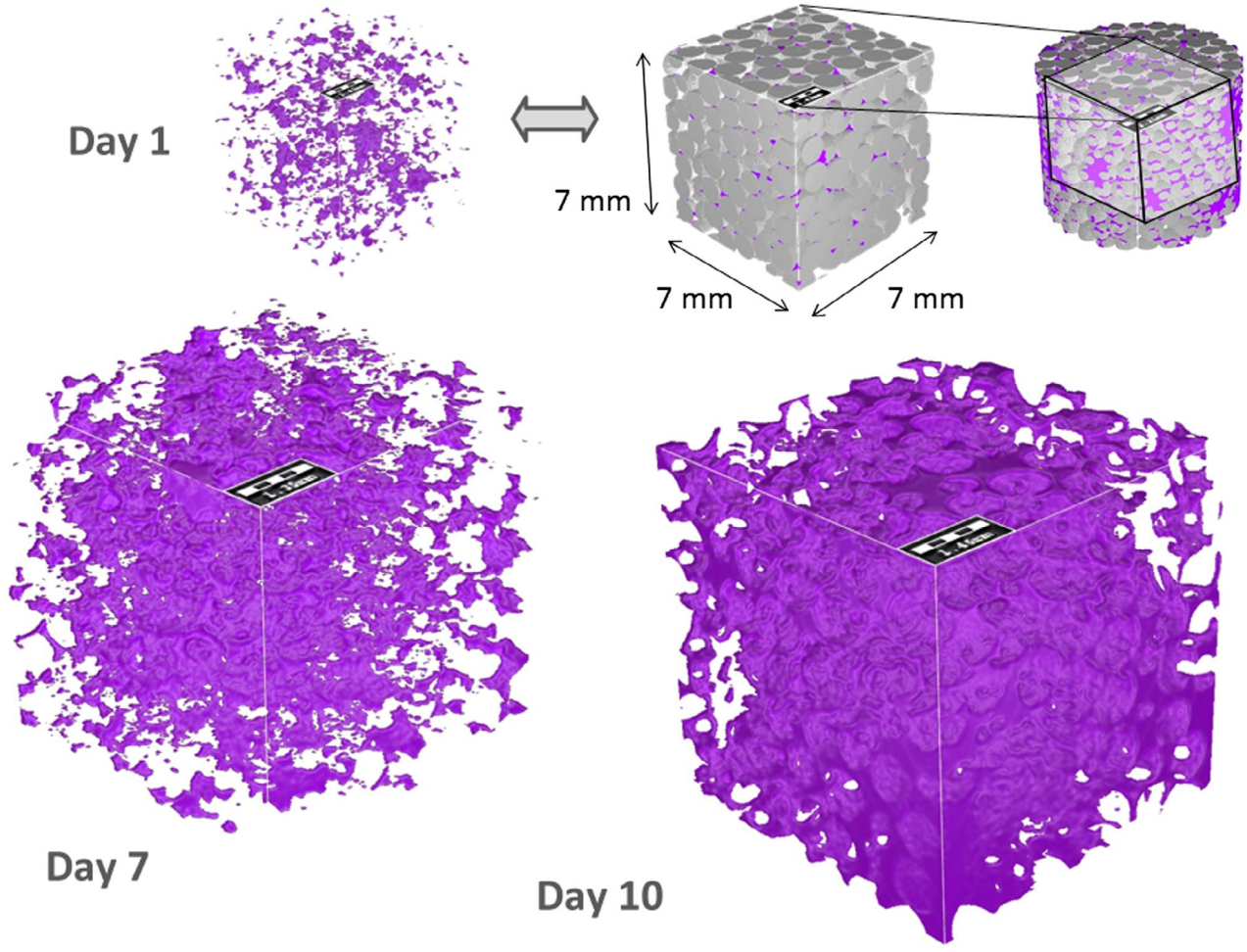

Figure 5. 3-D reconstruction of *P. putida* biofilms structure at three different growth stages in columns of 1 mm glass beads.

the accumulated bacterial biomass was visible as a blur at the bottom (inlet) of the column (Figure 2). From days 6 to 7 the biofilm started to be visible as opaque white-yellow formation and from day 7 the biofilm was clearly visible as an opaque formation localized at the bottom of the column. The experiments were usually stopped between days 7 and 10 of biofilm growth, when air bubbles started to appear, as this was considered to be the end of ideal growth conditions. The bubbles were assumed to be a product of biofilm respiration. They remained trapped in the biofilm structure when the biofilm was mature.

Effect of CN injection at the boundary of the columns

After image reconstruction and analysis, a validation of the biofilm-phase identification described above was carried out. The initial assumption was that CN pushed out water from the columns, leaving the biofilm intact. To verify this assumption, the CN injection protocol was investigated on a glass beads column at day 0; the biofilter was prepared using the same protocol as described previously and CN was injected without a prior incubation period. The biofilter was scanned and image segmentation was performed as described above.

The 3-D views at day 0 presented in Figure 4 reveal an edge effect, whereby biofilm is detected at the bead/column interface (Figure 4), regardless of the diameter of the beads. Since the part detected as biofilm cannot be real biofilm, the part recognized as biofilm must therefore be an artifact produced by the filling of contrast agent (CN). During its introduction in the column, CN is assumed to have replaced the aqueous medium entirely, but apparently some aqueous medium has remained trapped at the bead/column interface and to a lesser extent at the bead/bead interface. This phenomenon increased with the ratio between the bead diameter and the inner diameter of the column (Figure 4). The larger the beads, the more heterogeneous the flow would be and especially at the edges of the columns. In the case of the biofilter filled with 1 mm beads, this represents about 1.5% of the biofilm volume fraction of the entire column.

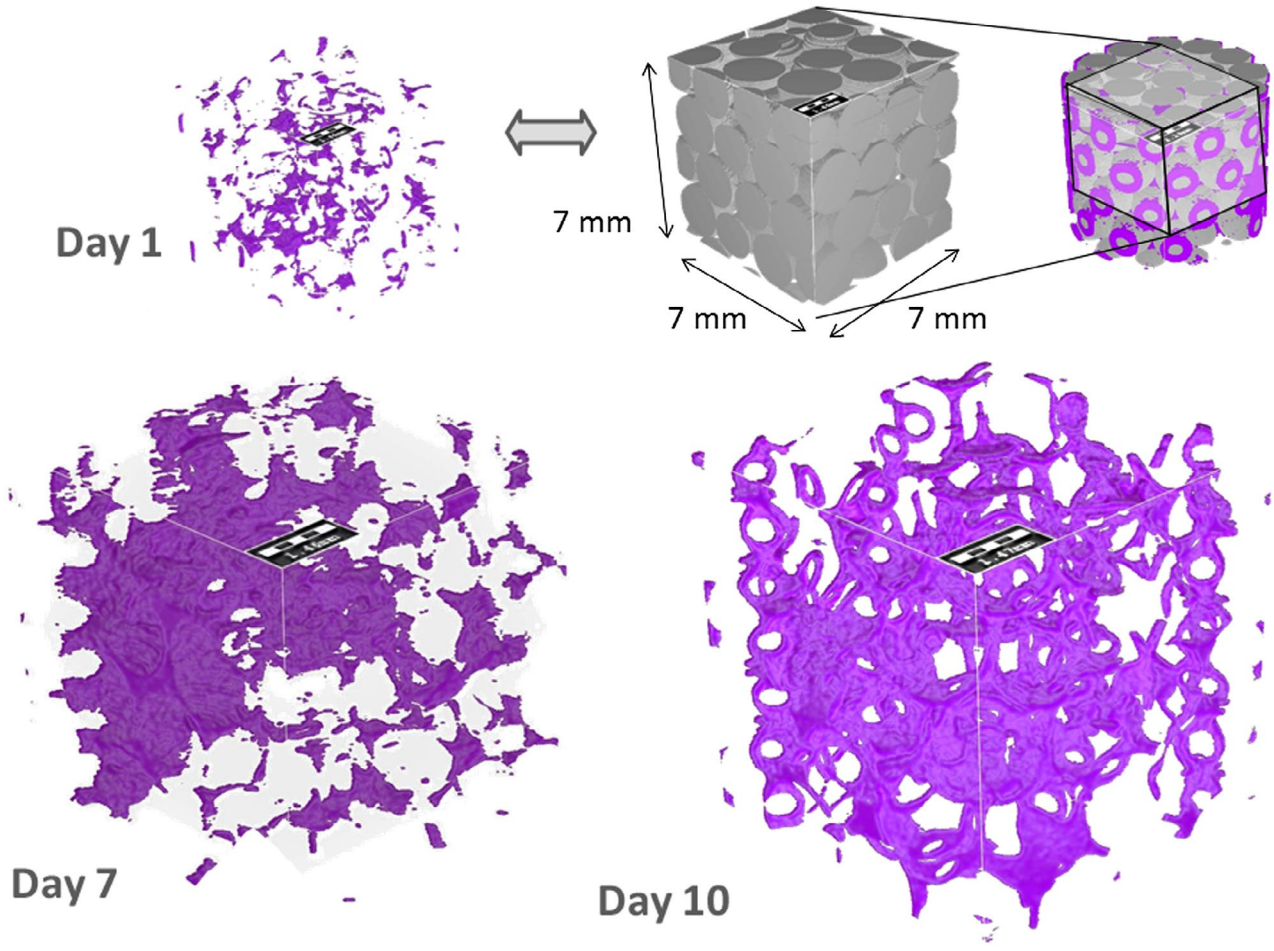

Figure 6. 3-D reconstruction of *P. putida* biofilm structure at three different growth stages in columns of 2 mm glass beads.

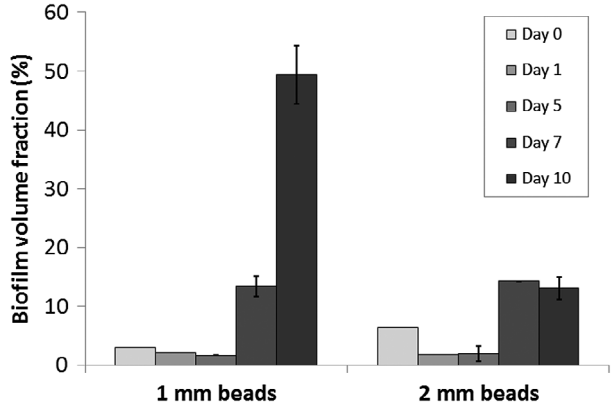

Figure 7. Temporal evolution of the volume fraction of *P. putida* biofilms grown in mini biofilters filled with 1 and 2 mm beads.

For seven-day-grown biofilms (Figure 4), the biofilm phase seems thicker around the inner edges of the columns, and after 10 days, the biofilm occupied large proportions of the column pore space. This analysis performed on 3-D images was confirmed by a visual inspection of the outer part of the column.

Consequently, to avoid any mistake in biofilm quantification linked to this side effect, especially at the early growth stages, a volume called region of interest (ROI) of $7 \times 7 \times 7$ mm^3 centered in the middle of the column was considered for further analysis (Figure 5). The representativity of this volume for both volume fractions of beads and of biofilm was checked according to the method proposed in Rolland du Roscoat et al. (2007).

Effect of chloronaphthalene injection on biofilm volume fraction at different growth stages

Biofilm growth was analyzed in the ROI in columns filled with 1 or 2 mm beads. At days 0 and 1, as previously mentioned, the biofilm phase detected by tomography (Figures 5–7) was attributed to nutrient medium trapped during contrast agent injection since no biofilm growth was detected in the columns (confirmed visually). This is in agreement with the edge effect described above, and was more pronounced in the 2 mm bead column (day 0, Figure 7). At day 5, regardless of the bead diameter, the biofilm fraction was quite low (< 5%) although biomass

Table 1. Main experimental conditions and parameter values for the biofilm volume fraction calculation from 3-D images of *P. putida* biofilms grown for seven or 10 days in columns filled with 1 mm glass beads.

Sample name	Biofilm age(days)	Resolution (µm)	Scan order	Data processing	Biofilm volume fraction (%)	Mean biofilm volume fraction
A	7	10.08	Scan 1	Operator A	14.6	12.9 ± 1.6
A1	7	10.08	Scan 2	Operator B	11.4	
A2	7	10.08	Scan 2	Operator A	12.7	
B	7	10.02	Scan 1	Operator A	12.6	12.2 ± 0.8
B1	7	10.02	Scan 2	Operator B	12.8	
B2	7	10.02	Scan 2	Operator A	11.4	
C	10	10.02	Scan 1	Operator A	45.1	46.9 ± 1.5
C1	10	10.02	Scan 2	Operator B	48.0	
C2	10	10.02	Scan 2	Operator A	47.7	

could be visually observed in the column walls. At day 7, regardless of the bead diameter, the biofilm volume detected was considerably increased, by up to 15% (Figures 5–7). This was confirmed by visual observations: the biofilm phase was opaque, indicative of compactness. These observations indicated that the loading of contrast agent in the columns washed out the suspended biomass and loosely attached biofilm but encompassed the mature, compact and tightly attached biofilm.

From day 7 to day 10 the biofilm volume was significantly increased (50%) in the 1 mm bead system but not in the system with 2 mm beads (15%) (Figures 5 and 6). In the 1 mm bead biofilter, biofilm development seemed to increase by steadily, occupying the empty pore space (Figure 5) and gaining in volume. In the 2 mm bead biofilter, the biofilm was randomly arranged at day 7 while at day 10 the biofilm seemed to encompass the beads and probably modeled itself to flow channels (Figure 6). So, although the biofilm structure looks very different when grown in 1 or 2 mm beads (between days 7 and 10) the volume fraction was similar. This is probably due to the larger size of the pores in the 2 mm bead porous medium, which would tend to increase the heterogeneity of biofilm development. This emphasizes either the importance of the size of the beads in the porous medium or the shear induced by water flow. The results indicate that the use of 1 mm beads induces a more homogeneous biofilm development in the porous medium. Consequently, further focus will be on the 1 mm bead biofilter. At this point the major limitations of the methodology described were identified: at early stages of growth biofilms cannot accurately be visualized and quantified because (1) the contrast agent injection washed out some of the loosely attached biofilm phases and (2) a proportion of the aqueous medium remained trapped in the system and was thus accounted for as biofilm. Reliable visualization and quantification of biofilm phases were obtained only at late growth stages (>7 days), when biofilms were compact, tightly attached and significantly enlarged in volume. It should also be noted that the differentiation between biofilm and CN during image analysis was also much simpler and more accurate with biofilters measured at later growth stages, with more mature biofilms.

Reproducibility and error in image manipulation

Another important question was that of reproducibility, in order to know whether the two biofilms grown for the same duration in independent experiments could be comparably analyzed and quantified. For that, biofilms were grown in two separate columns for seven days (columns A and B, Table 1) and one column for 10 days (column C). Since the columns were grown in separate experiments, different initial bacterial culture and nutrient medium were used. All columns were scanned at an identical location (20 mm height from the inlet) and biofilm volume fractions were quantified and compared. This study was restricted to beads 1 mm in diameter and was carried out in the ROI described in the previous section. Table 1 summarizes the differences observed between the biofilm samples.

Images acquired by laboratory tomograph always differed in quality from scan to scan due to the possible variation in the X-ray spot size and the environmental conditions of the room in which the tomograph was placed (Limodin et al. 2011). Therefore, each column was scanned twice (scans 1 and 2). Moreover, as described in the image processing treatment section, a threshold has to be manually chosen and can be user dependent. Two different users performed the segmentation procedure. Therefore, to investigate the influence of the data acquisition on the biofilm quantification results, the following procedure was applied for columns A, B and C. Columns were imaged by X-ray microtomography twice, ie there was about 10 min between the two consecutive scans. The scans were reconstructed independently to obtain datasets A1 and A2, B1 and B2 and C1 and C2. The image treatment procedure was applied independently on the 2nd scan of each column by a different user to obtain A3, B3 and C3. The volume fractions of biofilm determined for each case are presented in Table 1**.** Comparisons of the obtained results for each column individually (A/A1/A2;

B/B1/B2; C/C1/C2) suggested that differences between two scans of the same location in the column (A/A1, B/B1 and C/C1) resulted from image acquisition quality. In general, when there was more noise in the datasets, the threshold value was chosen to reduce the noise, affecting the calculated biofilm volume. Differences between separate image reconstructions of the same sample (A1/A2, B1/B2, C1/C2) were again the result of thresholding, but related to the operator manipulations rather than to image quality. Also, depending on image quality, median filter values varied, again causing differences in the calculated final biofilm volumes. Table 1 summarizes the biofilm volume fraction in each condition. From the three measurements obtained for the same column, it can be estimated that the error made on the quantification of the biofilm volume fractions, appeared to be reasonably low (<5%).

When the results from different columns grown for the same time period (A and B) are compared, the calculated biofilm volume fractions (Table 1) were similar for both columns. The small variation in this parameter can be attributed to the natural heterogeneity of biofilm formation. It can therefore be concluded that the protocol is reliable for a given condition of growth. When considering the influence of time and comparing between biofilm growth for seven and 10 days, a significant increase in biofilm volume fraction can be noticed (from 12.6 ± 1.2 to 46.9 ± 0.8). This is consistent with the visual observation of the biofilms inside the columns. Considering the heterogeneity of biofilm growth at the pore scale, this validates the reproducibility of biofilm growth, visualizations and the quantifications obtained by the method described herein.

The results of the present study on the possibility of reproducibly growing and imaging bacterial biofilms are in agreement with Bozorg et al. (2012) who tested this reproducibility by using bioluminescence imaging in small glass bead systems (450–600 μm in size). They imaged biofilms of *Pseudomonas fluorescens* grown for eight days in replicate and suggested that the biofilm growth in porous media and the images obtained were reproducible. The amount of biofilm was not quantified, but bioluminescence images showed significant amounts of biofilm at the same locations (ie the zone near the growth medium inlet) in each of the two replicates of the tested system.

Comparison to literature data

All previous studies intending to image bacterial biofilms (Iltis et al. 2011; Davit et al. 2011; Rolland du Roscoat et al. 2014) relied on the use of contrast agents, which can bias the analysis. However, despite the fact that the X-ray exposure coupled with 1-chloronaphthalene as a contrast agent doubtlessly destroys bacterial populations (in the present experiments also), it can be concluded that biofilms grown under identical conditions will present a similar and reproducible spatial structure. The biofilm growth in the present porous media was thus monitored by imaging separate samples and considering the biofilm growth to be continuous. Although the spatial arrangement of the biofilm and the position of the flow channels differed from sample to sample (as expected), the values of biofilm volume fraction, derived from X-ray tomography, were clearly reproducible, especially for mature biofilms (>seven days). The problem of injection of a contrast agent in the dead zones, as mentioned by Iltis et al. (2011), was eliminated by using CN as a contrast agent and making measurements in a restricted region of interest in the center of the column. The arrangement of CN was likewise limited to flow channels, but since image analysis interpreted anything that was not CN as a biofilm, dead end pores were also interpreted as biofilm volume, not as bulk liquid.

To the authors' knowledge most of the 3-D images of biofilms in porous media available in the literature were made with synchrotron X-ray microtomography. The 3-D datasets obtained with a synchrotron source (Iltis et al. 2011; Rolland du Roscoat et al. 2014) are in general more sensitive to small changes in density and are less noisy. However, the difficulty of accessing synchrotron instruments means that it is not possible to check reproducibility. The results presented here indicate that both biofilm growth and the 3-D images obtained *via* lab-based X-ray tomography are reproducible and can serve as a basis for testing different models of biofilm growth in porous media. Moreover, the study of both the reproducibility and the error in image treatment indicate that a single biofilter may be enough to give reliable quantification of biofilm volumes, thus validating previous studies conducted with single column systems.

Conclusions

The present study proposed and validated what can be considered as the first protocol for biofilm production as well as quantitative measurements coming from X-ray tomography and image analysis of its evolution at different stages of growth in simple porous media (columns of 10 mm inner diameter and 20 cm height filled with glass beads 1 or 2 mm in diameter). Some limitations for biofilm quantification relating to the use of a non-aqueous contrast agent were also overcome: a volume of about 7 × 7 × 7 mm^3 in the center of the porous medium was investigated provided that small glass beads (<1 mm in diameter) are used. A limitation that was not overcome with this procedure was the reliable and reproducible visualization of very young biofilms (less than three days) due to the

injection of the organic contrast agent, since it causes the detachment of loosely attached biofilm fragments which dominate at the early stages biofilm growth. With compact biofilms, tightly attached and significantly enlarged in volume, the procedure described herein allows biofilm volume to be measured reliably.

The temporal evolution of bacterial biofilm structure was recorded by imaging biofilms grown for different periods of time. Biofilm growth in porous media was reproducible and the data obtained were statistically relevant. The results presented here indicate that reproducible biofilm growth and 3-D images can be obtained *via* X-ray microtomography. These results constitute a good basis for testing and improving mathematical models describing biofilm growth in porous media, which are necessary for water treatment or soil remediation management.

Acknowledgements

The authors gratefully acknowledge Erwann Vince for technical help and support. This work benefited from the technical microbiology facilities of the MOME platform located at LTHE UMR 5564, Grenoble, France.

Disclosure statement

No potential conflict of interest was reported by the authors.

Funding

This work was supported by the LabEx Tec 21 [Investissements d'Avenir – grant agreement no ANR-11-LABX-0030]. LTHE is part of the Labex OSUG@2020 (ANR10 LABX56).

References

Beyenal H, Lewandowski Z, Harkin G. 2004. Quantifying biofilm structure: facts and fiction. Biofouling. 20:1–23. doi:http://dx.doi.org/10.1080/0892701042000191628

Billings N, Birjiniuk A, Samad TS, Doyle PS, Ribbeck K. 2015. Material properties of biofilms – a review of methods for understanding permeability and mechanics. Rep Prog Phys. 78(3):036601. doi:http://dx.doi.org/10.1088/0034-4885/78/3/036601

Bozorg A, Gates ID, Sen A. 2012. Real time monitoring of biofilm development under flow conditions in porous media. Biofouling. 28:937–951. doi:http://dx.doi.org/10.1080/08927014.2012.723204

Bridier A, Briandet R, Thomas V, Dubois-Brissonnet F. 2011. Resistance of bacterial biofilms to disinfectants: a review. Biofouling. 27:1017–1032. doi:http://dx.doi.org/10.1080/08927014.2011.626899

Davit Y, Iltis G, Debenest G, Veran-Tissoires S, Wildenschild D, Gerino M, Quintard M. 2011. Imaging biofilm in porous media using X-ray computed microtomography. J Microsc. 242:15–25. doi:http://dx.doi.org/10.1111/jmi.2011.242.issue-1

Durham DR, Marshall LC, Miller JG, Chmurny AB. 1994. Characterization of inorganic biocarriers that moderate system upsets during fixed-film biotreatment processes. Appl Environ Microbiol. 60:3329–3335.

Espinal P, Martí S, Vila J. 2012. Effect of biofilm formation on the survival of *Acinetobacter baumannii* on dry surfaces. J Hosp Infect. 80:56–60. doi:http://dx.doi.org/10.1016/j.jhin.2011.08.013

Graf von der Schulenburg DA, Pintelon TRR, Picioreanu C, Van Loosdrecht CM, Johns ML. 2009. Three-dimensional simulations of biofilm growth in porous media. AIChE J. 55:494–504. doi:http://dx.doi.org/10.1002/aic.v55:2

Hogan D, Kolter R. 2002. Why are bacteria refractory to antimicrobials? Curr Opin Microbiol. 5:472–477. doi:http://dx.doi.org/10.1016/S1369-5274(02)00357-0

Iltis GC, Armstrong RT, Jansik DP, Wood BD, Wildenschild D. 2011. Imaging biofilm architecture within porous media using synchrotron-based X-ray computed microtomography. Water Resour Res. 47:W02601 doi:http://dx.doi.org/10.1029/2010WR009410

Karrabi M, Séchet P, Morra C, Cartellier A, Geindreau C, Martins JMF. 2011. Investigation of hydrodynamics/biofilm growth coupling in a pilot scale granular bioreactor at low pore Reynolds number. Chem Eng Sci. 66:1765–1782. doi:http://dx.doi.org/10.1016/j.ces.2011.01.010

Limodin N, Réthoré J, Adrien J, Buffière JY, Hild F, Roux S. 2011. Analysis and artifact correction for volume correlation measurements using tomographic images from a laboratory X-ray source. Exp Mech. 51:959–970. doi:http://dx.doi.org/10.1007/s11340-010-9397-4

Majumdar U, Alexander T, Waskar M, Dagaonkar MV. 2014. Effect of biofilm on colloid attachment in saturated porous media. Water Sci Technol. 70:241–248. doi:http://dx.doi.org/10.2166/wst.2014.197

Meideros A. 2016. Experimental study of biofilms growth under controlled hydrodynamic conditions [PhD thesis]. France: Univeristy of Grenoble-Alpes.

Nicolella C, van Loosdrecht MCM, Heijnen JJ. 2000. Wastewater treatment with particulate biofilm reactors. J Biotechnol. 80:1–33. doi:http://dx.doi.org/10.1016/S0168-1656(00)00229-7

Patenge N, Arndt K, Eggert T, Zietz C, Kreikemeyer B, Bader R, Nebe B, Stranak V, Hippler R, Podbielski A. 2012. Evaluation of antimicrobial effects of novel implant materials by testing the prevention of biofilm formation using a simple small scale medium-throughput growth inhibition assay. Biofouling. 28:267–277. doi:http://dx.doi.org/10.1080/08927014.2012.671305

Rajbir S, Debarati P, Rakesh KJ. 2006. Biofilms: implications in bioremediation. Trends Microbiol. 15:389–397.

Rolland du Roscoat S, Decain M, Thibault X, Geindreau C, Bloch JF. 2007. Estimation of microstructural properties from synchrotron X-ray microtomography and determination of the REV in paper materials. Acta Mater. 55:2841–2850. doi:http://dx.doi.org/10.1016/j.actamat.2006.11.050

Rolland du Roscoat S, Martins JMF, Séchet P, Vince E, Latil P, Geindreau C. 2014. Application of synchrotron X-ray microtomography for visualizing bacterial biofilms 3D microstructure in porous media. Biotechnol Bioeng. 111:1265–1271. doi:http://dx.doi.org/10.1002/bit.25168

Salama Y, Chennaoui M, Sylla A, Mountadar M, Rihani M, Assobhei O. 2015. Characterization, structure, and function

of extracellular polymeric substances (EPS) of microbial biofilm in biological wastewater treatment systems: a review. Desalin Water Treat. 57(35):16220–16237. doi:http://dx.doi.org/10.1080/19443994.2015.1077739

Shafahi M, Vafai K. 2009. Biofilm affected characteristics of porous structures. Int J Heat Mass Transf. 52:574–581. doi:http://dx.doi.org/10.1016/j.ijheatmasstransfer.2008.07.013

Stewart PS, Costerton JW. 2001. Antibiotic resistance of bacteria in biofilms. Lancet. 358:135–138. doi:http://dx.doi.org/10.1016/S0140-6736(01)05321-1

Stoodley P, Dodds I, De Beer D, Scott D, Boyle J. 2005. Flowing biofilms as a transport mechanism for biomass through porous media under laminar and turbulent conditions in a laboratory reactor system. Biofouling. 21:161–168. doi:http://dx.doi.org/10.1080/08927010500375524

Vogt SJ, Sanderlin AB, Seymour JD, Codd SL. 2013. Permeability of a growing biofilm in a porous media fluid flow analyzed by magnetic resonance displacement-relaxation correlations. Biotechnol Bioeng. 110:1366–1375. doi:http://dx.doi.org/10.1002/bit.v110.5